REGULAR ARTICLE

blood advances

Platelet dense granules begin to selectively accumulate mepacrine during proplatelet formation

Hayley A. Hanby,[1-4] Jialing Bao,[1-3] Ji-Yoon Noh,[5] Danuta Jarocha,[6] Mortimer Poncz,[6] Mitchell J. Weiss,[7] and Michael S. Marks[1-3]

[1]Department of Pathology and Laboratory Medicine, Children's Hospital of Philadelphia, Philadelphia, PA; [2]Department of Pathology and Laboratory Medicine, [3]Department of Physiology, and [4]Cell and Molecular Biology Graduate Group, University of Pennsylvania, Philadelphia, PA; [5]Immunotherapy Convergence Research Center, Korea Research Institute of Bioscience and Biotechnology, Daejeon, Republic of Korea; [6]Division of Hematology, Department of Pediatrics, Children's Hospital of Philadelphia, Philadelphia, PA; [7]Department of Hematology, St. Jude Children's Research Hospital, Memphis, TN

Key Points

- Compartments labeled by the vital dense granule dye mepacrine are distinct from acidic structures in platelets but not in megakaryocytes.
- Distinct hypoacidic mepacrine-labeled structures first appear during megakaryocyte differentiation to proplatelets.

Platelet dense granules (DGs) are storage organelles for calcium ions, small organic molecules such as adenosine 5′-diphosphate and serotonin, and larger polyphosphates that are secreted upon platelet stimulation to enhance platelet activation, adhesion, and stabilization at sites of vascular damage. DGs are thought to fully mature within megakaryocytes (MKs) prior to platelet formation. Here we challenge this notion by exploiting vital fluorescent dyes to distinguish mildly acidic DGs from highly acidic compartments by microscopy in platelets and MKs. In isolated primary mouse platelets, compartments labeled by mepacrine, a fluorescent weak base that accumulates in DGs, are readily distinguishable from highly acidic compartments, likely lysosomes, that are labeled by the acidic pH indicator LysoTracker and from endolysosomes and α granules labeled by internalized and partially digested self-quenching BODIPY–labeled bovine serum albumin (DQ BSA). By contrast, in murine fetal liver and human $CD34^+$ cell-derived MKs and the megakaryocytoid cell lines, MEG-01 and differentiated G1ME2, labeling by mepacrine overlapped nearly completely with labeling by LysoTracker and partially with labeling by DQ BSA. Mepacrine labeling in G1ME2-derived MKs was fully sensitive to proton ATPase inhibitors but was only partially sensitive in platelets. These data indicate that mepacrine in MKs accumulates as a weak base in endolysosomes but is likely pumped into or retained in separate DGs in platelets. Fluorescent puncta that labeled uniquely for mepacrine were first evident in G1ME2-derived proplatelets, suggesting that DGs undergo a maturation step that initiates in the final stages of MK differentiation.

Introduction

Platelet dense granules (DGs) are secretory compartments within platelets that house small molecules such as adenosine 5′-diphosphate (ADP), Ca^{2+}, serotonin, and larger polyphosphates.[1,2] Effective hemostasis requires the release of DG contents upon platelet activation at sites of vascular damage. Consequently, defects in DG formation underlie δ storage pool deficiency in heritable hemorrhagic disorders such as Hermansky-Pudlak Syndrome (HPS).[3-5] The reduced accumulation of platelets during injury models in mouse models of HPS underscores a requirement for released DG contents in recruiting a platelet "shell" over a smaller DG-independent core, likely via ADP release and stimulation of P2Y receptors.[6-9] DGs are thought to form within megakaryocytes (MKs),[10] the nucleated precursor cells of platelets, but the mechanisms underlying DG formation and maturation are poorly understood, at least partially due to difficulties in definitively identifying DGs.

Submitted 14 March 2017; accepted 11 July 2017. DOI 10.1182/bloodadvances.2017006726.

The full-text version of this article contains a data supplement.

DGs in platelets are best visualized by whole-mount electron microscopy (EM) analysis as dense bodies[11] or by fluorescence microscopy following uptake of mepacrine, which accumulates preferentially in human, rat, and rabbit platelets.[12-20] Mepacrine also accumulates in DGs of mouse platelets, and its accumulation is reduced in platelets from mouse HPS models.[21-23] By contrast, it is not trivial to identify DGs by standard thin-section EM. DGs are named for their high lumenal calcium content,[24] making them electron dense in unstained whole-mount preparations. However, thin-section EM typically requires chemical fixation and contrast staining with reagents such as uranyl acetate or osmium tetroxide; small ions such as calcium do not survive fixation, and high concentrations of proteins, phospholipids, or nucleic acids in other structures such as α granules stain densely with these reagents.[25] This causes ambiguity in identifying DGs in standard thin-section electron micrographs of platelets.

The problem is compounded in large MKs in which whole-mount EM is not possible. Electron-dense "bulls-eye" structures in MK thin sections labeled with standard dyes or the uranaffin method (which labels biogenic amines[26]) have been interpreted as DGs,[10,27,28] but distinguishing these from the more abundant and heterogeneous α granules is challenging. Refinements in cryopreservation, specifically by high-pressure freezing and freeze substitution, have yielded platelet α granules more uniform in appearance and without an electron-dense core and therefore may be a promising avenue to distinguish granule populations in MKs,[29,30] but thus far dense granules have not been unambiguously identified by this technique. MKs also bear organelles that accumulate mepacrine.[28] However, in mouse MKs the intensity of mepacrine labeling per unit area is much lower than in platelets and is not further reduced significantly in HPS models.[22] Moreover, mepacrine-accumulating structures in a human MK-like cell line, MEG-01, are accessible to endocytic tracers,[31] as is expected for endolysosomal compartments but not for DGs. Mepacrine is a weak base that accumulates in lysosomes in other cell types.[32] Thus, whether mepacrine-labeled structures in MKs correspond to bona fide DGs or to endolysosomal compartments is not clear.

Here we use labeling with fluorescent vital dyes to show that whereas mepacrine labels distinct mildly acidic DGs in mouse platelets, mepacrine-labeled structures in MKs and MK-like cell lines are highly acidic and likely correspond to compartments of the late endolysosomal pathway. We further show that structures uniquely labeled by mepacrine and not by acidotropic dyes are first observed in a fraction of proplatelets that differentiate from MKs in vitro. Our data suggest that DGs either are not formed or are immature in MKs and do not mature until proplatelet formation, and have profound implications for understanding the timing of the DG biogenesis defects that occur in HPS and other δ storage pool deficiencies.

Methods

Materials

Unless otherwise indicated, all chemicals were from Sigma-Aldrich or Fisher Scientific, and all culture reagents were from Life Technologies.

Cell culture and MK differentiation

Culture of the doxycycline (dox)-inducible *Gata1* shRNA-expressing murine embryonic stem cells, G1ME2, and differentiation toward the MK lineage was performed as described elsewhere.[33] Briefly, to initiate differentiation, G1ME2 cells were washed with Iscove modified Dulbecco medium (IMDM) to remove doxycycline and then resuspended in medium containing serum-free IMDM supplemented with 25% F12, N2 supplement, B27 supplement without vitamin A, 7.5% bovine serum albumin (BSA), 0.75% L-glutamine, 100 ng/mL murine Stem Cell Factor (SCF; Peprotech), and 20 ng/mL murine thrombopoietin (TPO; Peprotech). Cells were cultured 3-4 days for MK analysis and 5-6 days for proplatelet analysis. HeLa cells were cultured in Dulbecco's modified Eagle medium with 10% heat-inactivated fetal bovine serum (FBS) and 5% L-glutamine. MEG-01 cells (American Type Culture Collection [ATCC] CRL-2021) were cultured in RPMI-1640 with 10% heat-inactivated FBS. Granulocyte colony-stimulating factor-mobilized human $CD34^+$ hematopoietic cells (HPCs), purchased from the Fred Hutchinson Cancer Research Center Hematopoietic Cell Processing and Repository Core, were differentiated into MKs for 12 days in 80% IMDM (Invitrogen), 20% BSA/insulin/transferrin serum substitute (Stem Cell Technologies), 20 μg/mL low-density lipoprotein (CalBiochem), and 100 μM 2-mercaptoethanol (Sigma-Aldrich), with the following recombinant human cytokines added: SCF (1 ng/mL), TPO (100 ng/mL), interleukin-9 (13.5 ng/mL), and interleukin-6 (7.5 ng/mL).

Isolation of platelets and fetal liver-derived megakaryocytes

Platelets were prepared as has been described.[34,35] Briefly, blood was drawn from 6-week-old C57BL/6 mice by cardiac puncture and collected into citrate-dextrose solution (ACD; 85 mM sodium citrate, 111 mM glucose, 71 mM citric acid) with 0.1 μM prostaglandin E1. Whole blood was fractionated by centrifugation for 10 min at 100*g*, and platelet-rich plasma (PRP) was collected into a clean tube; the remaining blood was washed with ACD/prostaglandin E1 solution and repelleted to collect more PRP. The pooled PRP was centrifuged at 400*g* for 10 min to pellet the platelets. The pellet was then resuspended in modified *N*-2-hydroxyethylpiperazine-*N*′-2-ethanesulfonic acid (HEPES)–Tyrodes buffer (12 mM NaHCO3, 138 mM NaCl, 5.5 mM glucose, 2.9 mM KCl, 10 mM HEPES containing 0.1% BSA, 1mM $CaCl_2$, 1mM $MgCl_2$, pH 7.4) and used immediately.

Fetal liver (FL)–MK were prepared as described.[22,33] Briefly, fetal livers were obtained from pups harvested from E12 to E14 timed pregnant C57BL/6 mice. Pooled, isolated livers were briefly homogenized, and a single cell suspension was made by drawing the cells into a syringe through a 25-gauge needle and then expelling the cells through a 100-μm filter. The hematopoietic progenitors were enriched by depletion of other cell types by using a cocktail of biotinylated antibodies to nonhematopoietic and nonprogenitor cells (CD5, CD11b, CD19, CD45R/B220, Ly6G/C(Gr-1), TER119, 7-4) and streptavidin-coated magnetic particles (Stemcell Technologies). Progenitor cells were then differentiated by culture for 5-7 days in IMDM, supplemented with 10% FBS, 1% murine SCF conditioned medium, 0.5% murine TPO, penicillin/streptomycin, and L-glutamine. Matured MKs were purified on a BSA gradient.

All animal work was conducted with approval from the Institutional Animal Care and Use Committee of the Children's Hospital of Philadelphia.

Mepacrine uptake, acidic compartment staining, and fluorescence microscopy

For imaging, 35-mm glass-bottom dishes with No. 1.5 glass thickness (MatTek) were coated with 15 μg/mL fibronectin in Dulbecco's

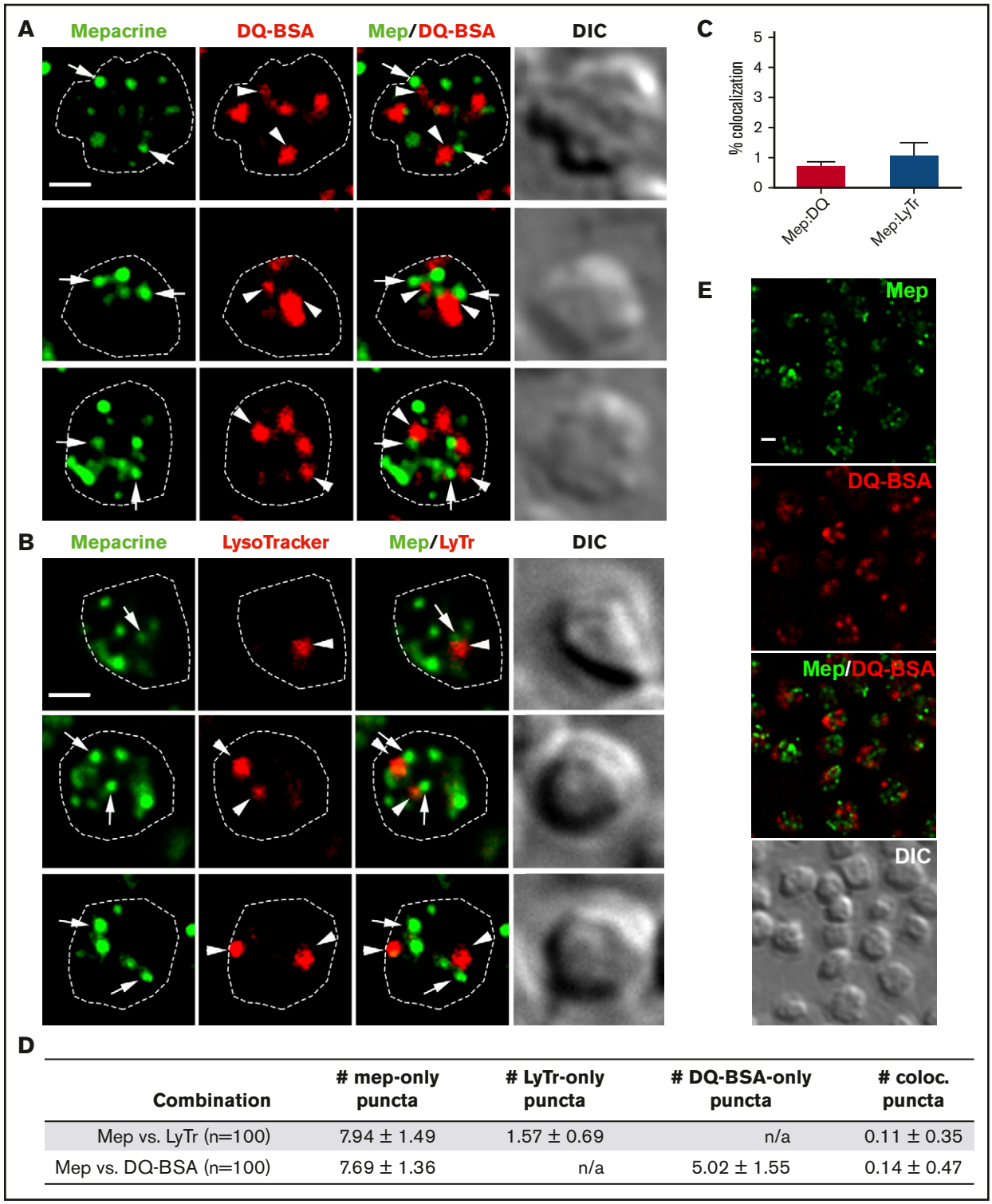

D

Combination	# mep-only puncta	# LyTr-only puncta	# DQ-BSA-only puncta	# coloc. puncta
Mep vs. LyTr (n=100)	7.94 ± 1.49	1.57 ± 0.69	n/a	0.11 ± 0.35
Mep vs. DQ-BSA (n=100)	7.69 ± 1.36	n/a	5.02 ± 1.55	0.14 ± 0.47

Figure 1. Mepacrine accumulates in structures distinct from lysosomes in platelets. (A-B) Shown are deconvolved, single-plane images from a *z*-series image stack of 3 individual platelets labeled with each combination individually or together (merge), along with a corresponding differential interference contrast image (DIC). Puncta are labeled by mepacrine (arrows) or by DQ BSA or LysoTracker (arrowheads). The cell outline is based on the DIC image (white dotted line). Scale bars, 1 μm. Platelets were incubated with 50 μM mepacrine (green) and either 10 μg/mL DQ BSA (red; A) or 200 nM LysoTracker Red DND-99 (red; B) for 30 min and analyzed by fluorescence microscopy. (C-D) Quantification of both the degree (mean ± SD) of mepacrine colocalization with DQ BSA or LysoTracker (N = 105 platelets each from 3 individual experiments) and the number of puncta per platelet (mean ± SD) labeled by mepacrine alone (#mep-only), LysoTracker alone (#LyTr-only), DQ BSA alone (#DQ-BSA-only) or by both mepacrine/LysoTracker or mepacrine/DQ BSA (# coloc.). (E) Shown is a deconvolved, single-plane image of a field of platelets labeled with mepacrine (Mep, green) and DQ BSA (red) individually or merged, along with corresponding DIC image. Scale bar, 1 μm. Platelets were analyzed by wide field microscopy at room temperature with a

phosphate-buffered saline (DPBS) for 3 h (G1ME2, FL-MKs, HeLa, and MEG-01 cells) or 30 min to 1 h (platelets) at room temperature. Dishes were then washed once with DPBS and immediately plated with cells. MKs were plated 1 day before the experiment. To stain, we incubated cells with 50 μM mepacrine and 200 nM LysoTracker Red DND-99 or 10 μg/mL DQ Red BSA (self-quenching BODIPY–labeled bovine serum albumin [DQ BSA]) in the culture medium for 30 min at 37°C, 5% CO_2. Where indicated, cells were pretreated with 100 nM bafilomycin A_1 (bafA_1; Sigma-Aldrich) or 5 nM concanamycin B (Enzo) for 30 min. After incubation with fluorescent dyes, cells were washed with their respective media. For G1ME2-MKs and proplatelets, exceedingly gentle washing was necessary to prevent detachment, such that substantial excess dye remained in the cytoplasm. This contributed to the "haze" or diffuse staining seen throughout the cell body or proplatelet extension. Control experiments in which G1ME2 cells were labeled with mepacrine or LysoTracker Red alone were performed (not shown) to ensure no bleed-through of fluorescence during image acquisition. To distinguish MKs in G1ME2 culture (Figure 4B), CD41 was labeled with a rat monoclonal anti-mouse antibody (BioLegend) conjugated to Alexa Fluor 647 (using Labeling Kit by Invitrogen). Platelets, and in some cases proplatelets, were analyzed by wide-field microscopy using a Leica DM IRBE equipped with a 100× (platelets) or 63× (other cells) Plan Apochromat objective lens (Leica; both 1.4 NA), an Orca Flash 4 complementary metal-oxide-semiconductor (CMOS) camera (Hamamatsu Photonics), and Leica Application Suite software. In some cases, proplatelets were imaged by a spinning disk confocal microscopy using a Leica DMi8 inverted microscope equipped with an Orca Flash 4 CMOS camera (Hamamatsu Photonics), a 100× Plan Apochromat objective lens (Leica; 1.4 NA), and VisiVIEW imaging software (Visitron Systems). MKs were imaged by spinning disk confocal microscopy using either an Olympus IX71 inverted microscope equipped with an electron- multiplying charge-coupled device camera (EM-CCD; ImagEM, Hamamatsu Photonics) and MetaMorph (Molecular Devices) software, or an Ultraview inverted microscope (PerkinElmer) equipped with a 63× Plan Apochromat lens (Carl Zeiss), a CCD camera (Orca-ER, Hamamatsu Photonics), and Volocity software (PerkinElmer). Images were captured in sequential *z* planes. When imaging bafA_1- or concanamycin B–treated and untreated cells, acquisition settings (ie, exposure time and light intensity) were maintained identically for both groups. Wide-field images were deconvolved using 3 iterations of Gold's iterative deconvolution algorithm within the Leica Application Suite software. All images presented in the figures are of a single *z* plane, except for the 3D reconstruction of platelets in Figure 2, generated using the Leica Application Suite software.

Quantification of colocalization between fluorescent dyes and of stained puncta

Colocalization between 2 fluorescent dyes was quantified from raw single-plane images of cells using ImageJ. Briefly, binary fluorescence images were generated by subtracting the local background before thresholding with a sliding paraboloid. The Image Calculator function was used to multiply both binary images from pairwise dye labelings. The resulting image represents the area of overlap between the 2 dyes. The areas of labeling or overlap in structures larger than 0.05 microns were quantified using the Analyze Particles function; the ratio of overlap to total labeling gives the percentage of overlap. In MKs, percentages of overlap shown were normalized to the percentage of overlap between LysoTracker Red and LysoTracker Green in G1ME2-MKs (nearly 100%). Colocalization quantification likely underestimates the true degree of colocalization due to slight cell movement during image acquisition. Similarly, to quantify the number of puncta (single dye-only and colocalized) in cells, fluorescence images were processed for background subtraction with a sliding paraboloid, and then puncta were manually counted in single-plane images.

Quantification of change in signal intensity with bafilomycin A_1 treatment

For platelets, background dye labeling was not grossly affected by treatment with bafA_1. Thus, to measure the reduction in labeling intensity following bafA_1 treatment, the intensity of labeling over each platelet area was measured using the Measure function in ImageJ. Measurements were made from 35 individual platelets and an averaged background value (from an unlabeled area on the coverslip) was subtracted from each measurement in each experiment. Values represent pooled data from 3 different experiments (105 platelets each of treated and untreated platelets) and are normalized to the average intensity value of untreated control platelets as 100%.

Because background dye labeling in G1ME2-MKs (or HeLa cells) after bafA_1 or concanamycin B treatment was high, it was not possible to calculate absolute reductions in punctate signals after treatment. Thus, the difference in signal intensity of mepacrine or LysoTracker Red puncta in relation to background before and after treatment with bafA_1 or concanamycin B was quantified from raw single-plane images of G1ME2-MKs using ImageJ. Briefly, a 50 × 50 square pixel region within each cell (N = 30), excluding nuclei, was selected to measure the standard deviation of each dye's signal intensity. The average standard deviation value for each dye's signal intensity in bafA_1- or concanamycin B–treated cells was compared with untreated cells.

Statistical analysis

Statistical significance was determined by the unpaired, nonparametric, 2-tailed *t* test (Mann-Whitney; $^{**}P < .01$; $^{****}P < .0001$).

Results

Murine platelets exhibit distinct mepacrine-positive and acidic compartments

Mepacrine accumulates specifically in DGs and not lysosomes in human and mouse platelets,[13,14,22,36] and its accumulation is reduced by δ storage pool deficiency as in HPS.[21-23] To determine whether each compartment can be distinctly labeled by vital dyes in

Figure 1. (continued) Leica DM IRBE equipped with a 100× Plan Apochromat objective lens (1.4 NA), a Hamamatsu Orca Flash 4 digital CMOS camera, and Leica Application Suite software. Imaging medium was modified, calcium-free Tyrode's buffer. Deconvolution was performed in Leica Application Suite software using Gold's iterative deconvolution algorithm. Mepacrine has an excitation/emission of 436/525 nm; LysoTracker Red excitation/emission: 577/590 nm; DQ BSA excitation/emission: ~590/~620 nm. Coloc., colocalization; DIC, differential interference contrast; LyTr, LysoTracker; Mep, mepacrine; n/a, not applicable.

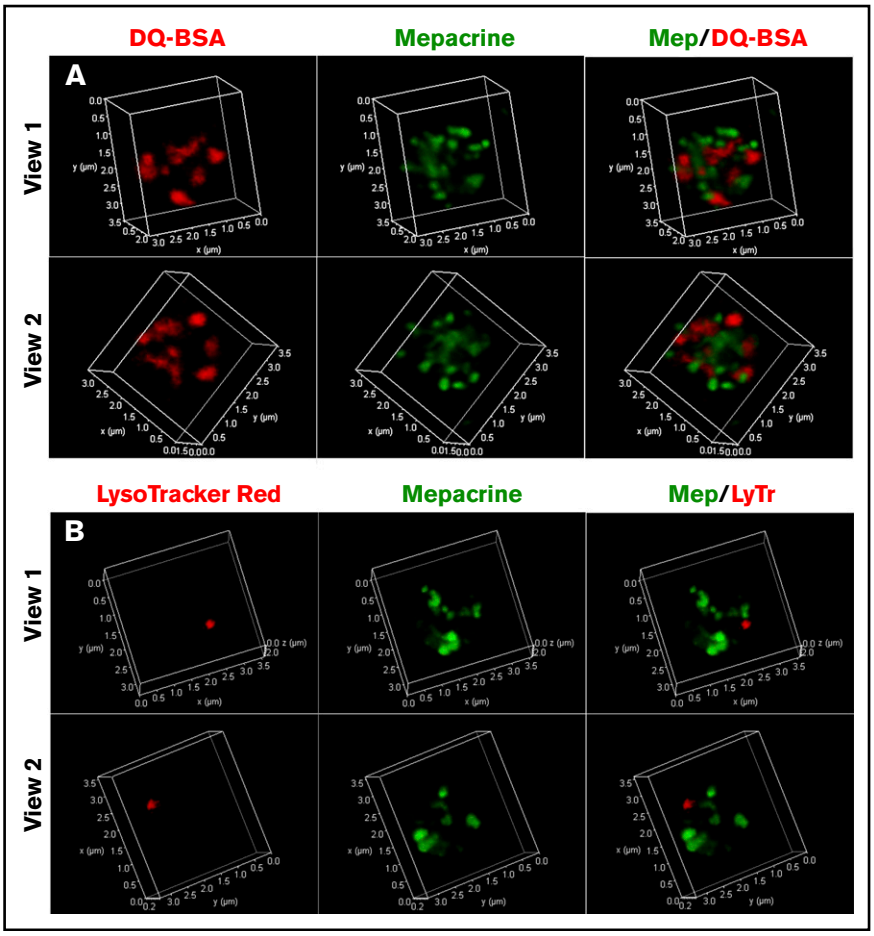

Figure 2. 3D reconstruction of labeled platelets. *Z* series of images of platelets shown in Figure 1 were subjected to 3D rendering to emphasize the distinct distribution of puncta labeled by DQ BSA (A; red) or LysoTracker Red DND-99 (B; red) from those labeled by mepacrine in 3D space. (A) Platelet from the first row of Figure 1A is shown in 2 views (view 1: 169°, −12°, −169° [X, Y, Z]; view 2: 8°, −12°, 141°). (B) Platelet from the first row of Figure 1B is shown in 2 views (view 1: −7°, 3°, 17°; view 2: −172°, −3°, 112°). The x- and y-axes are labeled for scale in micrometers. Three-dimensional reconstruction was performed with Leica Application Suite software.

mouse platelets, we incubated isolated platelets with mepacrine and either LysoTracker Red, which accumulates in acidic organelles following protonation, or DQ BSA, a self-quenching fluorophore-labeled bovine serum albumin derivative that fluoresces only when hydrolyzed by lysosomal proteases. Cells were then analyzed by fluorescence microscopy and deconvolution. In single-plane images, mepacrine displayed characteristic punctate staining with 6-10 puncta per platelet, whereas LysoTracker Red labeled 2-3 larger puncta per platelet and DQ BSA 4-6 larger puncta per platelet (Figure 1A-B shows examples of individual platelets; Figure 1E shows that all platelets in a field label similarly). Albumin can be either taken up into α granules (perhaps after limited proteolysis and unfolding) or delivered to lysosomes,[37] likely explaining the higher number of structures containing DQ BSA in comparison with LysoTracker. Accordingly, only a subset of DQ BSA–labeled puncta cosegregated with LysoTracker in platelets (supplemental Figure 1); the LysoTracker-negative puncta likely correspond to a subset of α granules. Importantly, neither LysoTracker Red nor DQ BSA demonstrated significant overlap with mepacrine (quantified in Figure 1C-D). Three-dimensional rendering of deconvolved images captured in successive image planes shows that all puncta were present within platelets and did not overlap in any plane (Figure 2). These data support previous conclusions that mepacrine labels DGs but not lysosomes (or α granules) in platelets.

The lumenal space of DGs is thought to be mildly acidic,[38,39] whereas lysosomes are thought to have a pH of ~4.5. If mepacrine accumulated in DGs merely as a weak base, then its accumulation should be antagonized by treatment with bafA$_1$, a vacuolar proton ATPase (vATPase) inhibitor that prevents acidification of endosomes and lysosomes. Indeed, pretreatment of platelets with 100 nM bafA$_1$ reduced labeling intensity by LysoTracker by 80%; however, the same treatment diminished the intensity of mepacrine puncta by significantly less (Figure 3A; quantified in Figure 3B). Similarly, treatment with another vATPase inhibitor, concanamycin B (5 nM), only partially eliminated mepacrine labeling (data not shown). These data indicate that mepacrine concentrates in DGs by a mechanism that is only partially acid dependent and confirms that mepacrine and LysoTracker can be used to distinguish between DGs and acidic endolysosomes in platelets.

Mepacrine concentrates in acidic compartments in MKs

We next tested whether mepacrine-labeled DGs are distinguishable from highly acidic endolysosomal compartments in MKs or megakaryocytoid cell lines. Fetal liver-derived mouse MKs (FL-MKs), the human megakaryocytoid cell line MEG-01, CD34$^+$ human HPC-derived MKs, and MKs induced by GATA1 derepression in the mouse G1ME2 hematopoietic progenitor cell line (G1ME2-MKs)[33] were incubated with mepacrine and LysoTracker Red and then analyzed by fluorescence microscopy. As was previously observed, mepacrine labeling was less intense in MKs than in platelets,[22] and because mepacrine also intercalates with DNA, nuclear labeling was apparent in most cells in addition to cytoplasmic puncta. Unlike

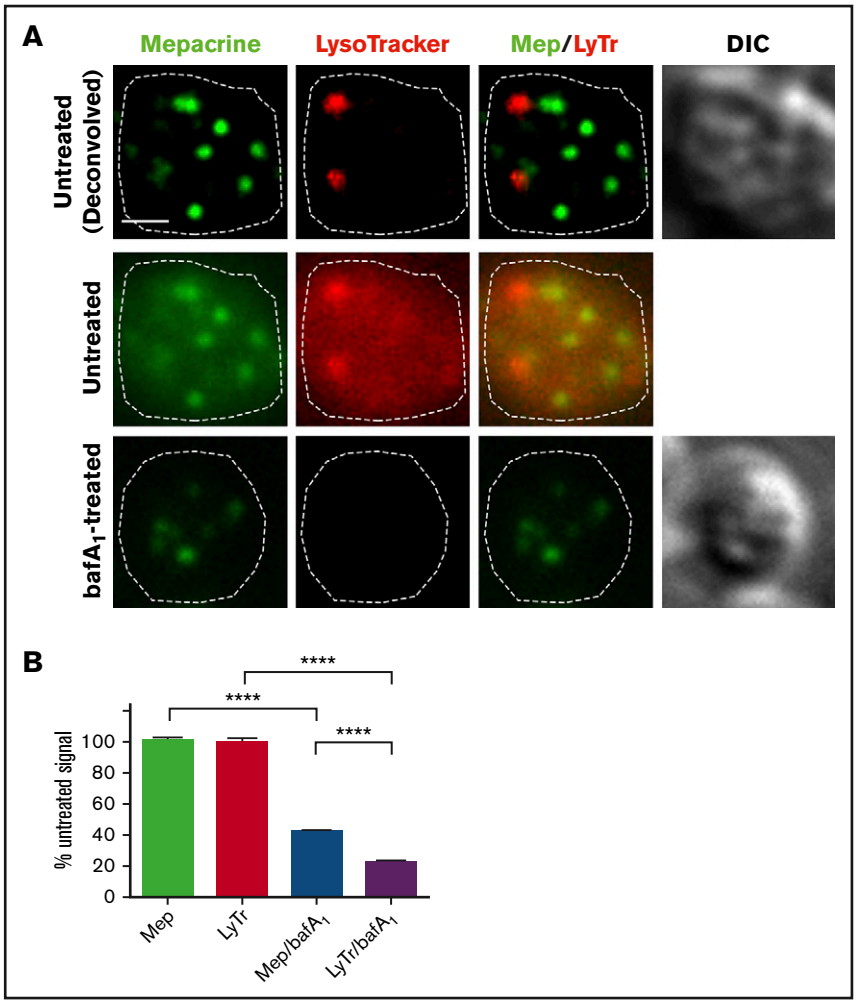

Figure 3. Mepacrine labeling is less sensitive to deacidification than LysoTracker labeling in platelets. (A) Platelets were pretreated with vehicle or with bafA$_1$ and then labeled with mepacrine (green) and LysoTracker Red DND-99 (red) together with vehicle or 100 nM bafA$_1$ for 30 min. Shown is a single-plane image of a single platelet from each treatment, showing each label alone or merged (Mep/LyTr) and the corresponding DIC image; the middle and lower panels are raw images, and the upper panels are deconvolved images of the middle panels. The cell outline is based on the DIC image (dotted line). Scale bar, 1 μm. (B) Quantification of fluorescence intensities of mepacrine or LysoTracker Red in control or bafA$_1$-treated cells (taken from raw images), expressed as a percentage of the untreated control (mean ± SD). N = 105 platelets from 3 separate experiments. Platelets were analyzed by wide-field microscopy at room temperature with a Leica DM IRBE equipped with a 100× Plan Apochromat objective lens (1.4 NA), a Hamamatsu Orca Flash 4 CMOS camera, and Leica Application Suite software. Imaging medium was modified, calcium-free Tyrode's buffer. Deconvolution was performed with Leica Application Suite software using 3 iterations of Gold's iterative deconvolution algorithm. Mepacrine has an excitation/emission of 436/525 nm; LysoTracker Red excitation/emission: 577/590 nm. ****$P < .0001$.

those in platelets, most mepacrine-positive puncta colocalized nearly completely with LysoTracker in each of the MK or MK-like cells (after normalization to 100% for overlap of LysoTracker Red with LysoTracker Green DND-26; Figures 4 and 5A,C-D). This suggests either that mepacrine-labeled DGs in MKs are not segregated from endolysosomes or that mepacrine accumulates in endolysosomes as a simple weak base, as has been previously shown in other cell types,[32] and not in separable DGs in MKs. Consistent with the latter, punctate labeling by both mepacrine and LysoTracker Red was equally abolished in G1ME2-MKs upon treatment with bafA$_1$ or concanamycin B (Figure 6A-C; supplemental Figure 2A-D), as is indicated by the reduced standard deviation of signal intensity throughout the MK cytoplasm (Figure 6D-E; supplemental Figure 2E-F). Graded dosing of concanamycin B showed that mepacrine labeling in G1ME2-MKs was at least as sensitive to concanamycin B as was Lysotracker labeling (supplemental Figure 2E-F), contrasting with the reduced sensitivity to bafA$_1$ in platelets (Figure 3). Similarly, bafA$_1$-sensitive accumulation of both mepacrine and LysoTracker Red was observed in the same puncta in undifferentiated G1ME2 megakaryocyte-erythroid progenitors and the nonhematopoietic cell line, HeLa, neither of which contains DGs (Figure 5B-D; supplemental Figure 3). Together, these data indicate that mepacrine does not label DGs or separable DG precursors in MKs but rather accumulates in acidic endolysosomal compartments. Consistently, mepacrine colocalized extensively with DQ BSA but only partially with internalized fibrinogen in MKs, which is sorted to α granules from multivesicular late endosomes and overlapped partially with DQ BSA and with LysoTracker Red[40] (supplemental Figure 4A-F); overlap of fibrinogen with DQ BSA fluorescence supports previous observations that partially digested BSA is also sorted to α granules from late endosomes in MKs.[37,40,41]

Separable DGs are first observed in a fraction of proplatelets

When do DGs acquire the ability to uniquely concentrate mepacrine? To test whether mepacrine begins to accumulate in structures distinct from endolysosomes during MK differentiation, we differentiated G1ME2 cells to MKs for 5-6 days, a point at which they generate long extensions that resemble proplatelets[33] (Figure 7A-B). The cells were then incubated with mepacrine and LysoTracker Red and analyzed by confocal fluorescence microscopy. In an effort to distinguish between proplatelet differentiation stages, proplatelets were characterized as detached or attached, depending on whether the proplatelet string obviously extended from a MK cell body within the plane of focus (with the caveat that

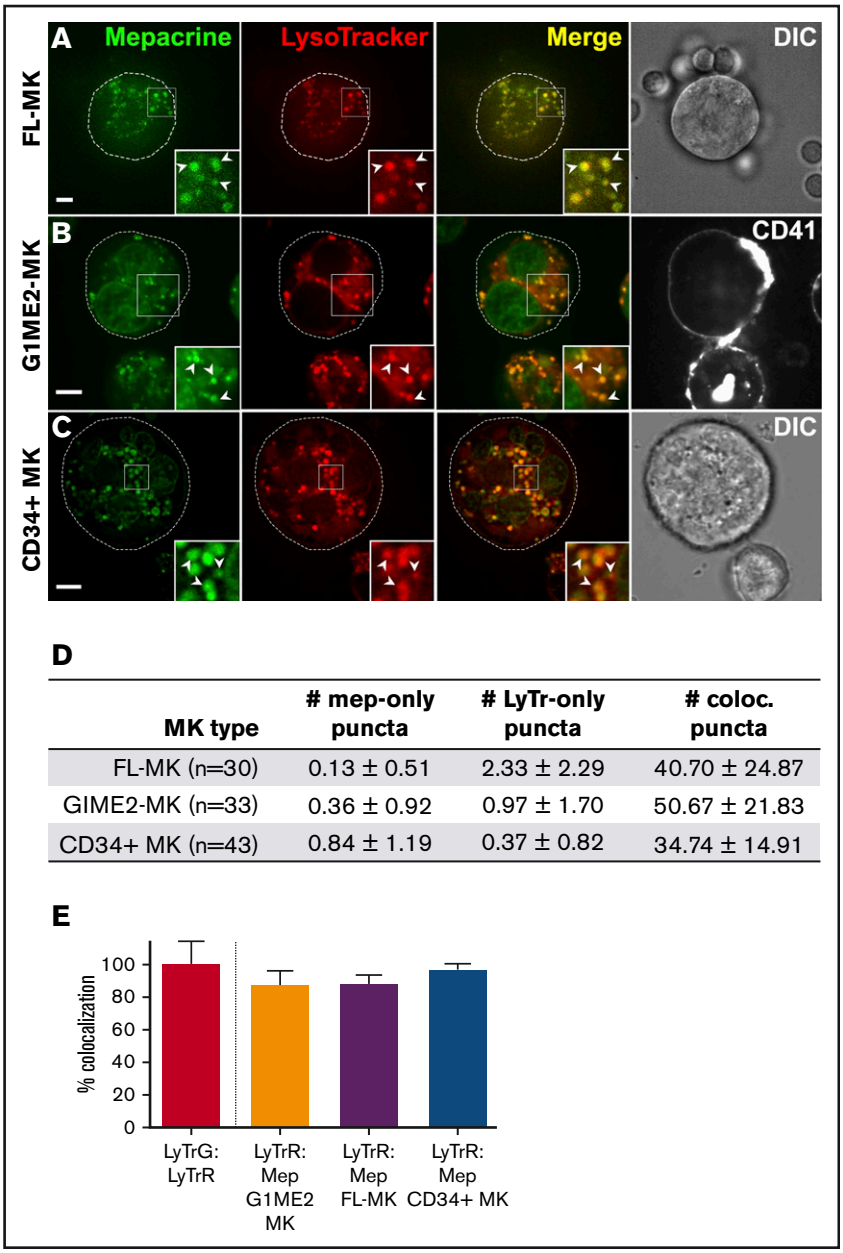

D

MK type	# mep-only puncta	# LyTr-only puncta	# coloc. puncta
FL-MK (n=30)	0.13 ± 0.51	2.33 ± 2.29	40.70 ± 24.87
GIME2-MK (n=33)	0.36 ± 0.92	0.97 ± 1.70	50.67 ± 21.83
CD34+ MK (n=43)	0.84 ± 1.19	0.37 ± 0.82	34.74 ± 14.91

E

Figure 4. Mepacrine labels acidic endolysosomes in MKs. Murine fetal liver-derived MKs (FL-MKs) (A,D-E), G1ME2 cells differentiated for 3-4 days to MKs (G1ME2-MK) (B,D-E), or human CD34-positive HPC-derived MKs ($CD34^+$ MK) (C-E) were incubated with 50 μM mepacrine (green) and 200 nM LysoTracker Red DND-99 (red) for 30 min; cells in panel B were also incubated with Alexa Fluor-647-conjugated anti-CD41 antibody. Images are of a single plane; panel C is deconvolved. In panels A and C, a corresponding DIC image is shown, and the cell outline is indicated by the dotted line (A-C). In panel B, CD41 labeling is also shown; ×2 magnification of boxed regions (insets); examples of overlap between mepacrine and LysoTracker (arrowheads). Scale bars, 5 μm. (D) The number (mean ± SD) of puncta per platelet labeled by mepacrine alone (#mep-only), LysoTracker Red alone (#LyTr-only), or both (#coloc.) in G1ME2-MK (n = 33), FL-MK (n = 30), and $CD34^+$ MK (n = 43). (E) Quantification of the percentage (mean ± SD) of mepacrine labeling that colocalized with LysoTracker Red labeling in each cell type (n = 33 G1ME2-MK; n = 30 FL-MK; n = 43 $CD34^+$ MK). Values are normalized to 100% for overlap of LysoTracker Red with LysoTracker Green DND-26 in G1ME2-MK (n = 79). Fetal-liver MKs were imaged by spinning-disk confocal microscopy at room temperature with an Olympus IX71 inverted microscope equipped with a Hamamatsu ImagEM EM-CCD camera, a 60× Plan Apo water immersion objective (1.2 NA), and MetaMorph software. G1ME2-MKs were imaged by spinning-disk confocal microscopy at room temperature with an Ultraview inverted microscope equipped with a 63× Plan Apochromat lens, a Hamamatsu Orca-ER CCD camera, and Volocity software. $CD34^+$ MKs were imaged by wide-field microscopy at room temperature with a Leica DM IRBE equipped with a 100× Plan Apochromat objective lens (1.4 NA), a Hamamatsu Orca Flash 4 CMOS camera, and Leica Application Suite software. Imaging medium was IMDM. Mepacrine has an excitation/emission of 436/525 nm; LysoTracker Red excitation/emission: 577/590 nm. LyTrG, LysoTracker Green; LyTrR, LysoTracker Red.

attachment sites might not have been visible). In swollen regions of both proplatelet types,[42] the majority of mepacrine-labeled puncta overlapped with LysoTracker labeling (Figure 7B-C). However, a few distinct puncta that labeled uniquely with mepacrine were also consistently observed (0.5 ± 1.4 [N = 30] vs 1.3 ± 2.5 [N = 42] mepacrine-only puncta/attached or detached proplatelet, respectively; Figure 7A [arrows], 7D; supplemental Figure 5). Although puncta that labeled only with mepacrine were more numerous among detached proplatelets, the difference was not statistically significant (P = .1288; unpaired, 2-tailed t test). More diffuse labeling was observed in proplatelets than in other cell types because of the reduced washing required to prevent proplatelet strings from washing away, but quantification was accomplished after local background subtraction to resolve this issue. These data indicate that DG-specific accumulation of mepacrine is initiated upon the onset of MK differentiation toward proplatelets and is likely completed after platelet formation.

Discussion

DGs have long been considered to be fully formed in MKs, because MKs accumulate serotonin in dense structures[26,43,44] and harbor a secretable pool of ADP.[45] However, our data suggest that this may not be the case. Our findings demonstrate that although mepacrine uniquely labels DGs in platelets, it incorporates only as a weak base into acidic endolysosomal organelles of MKs and that mepacrine-labeled structures in MKs do not necessarily become dense granules. Mepacrine-labeled structures that are distinct from acidic endolysosomes become evident only in proplatelets, which represent the final stage of MK maturation. These data have important implications for the timing

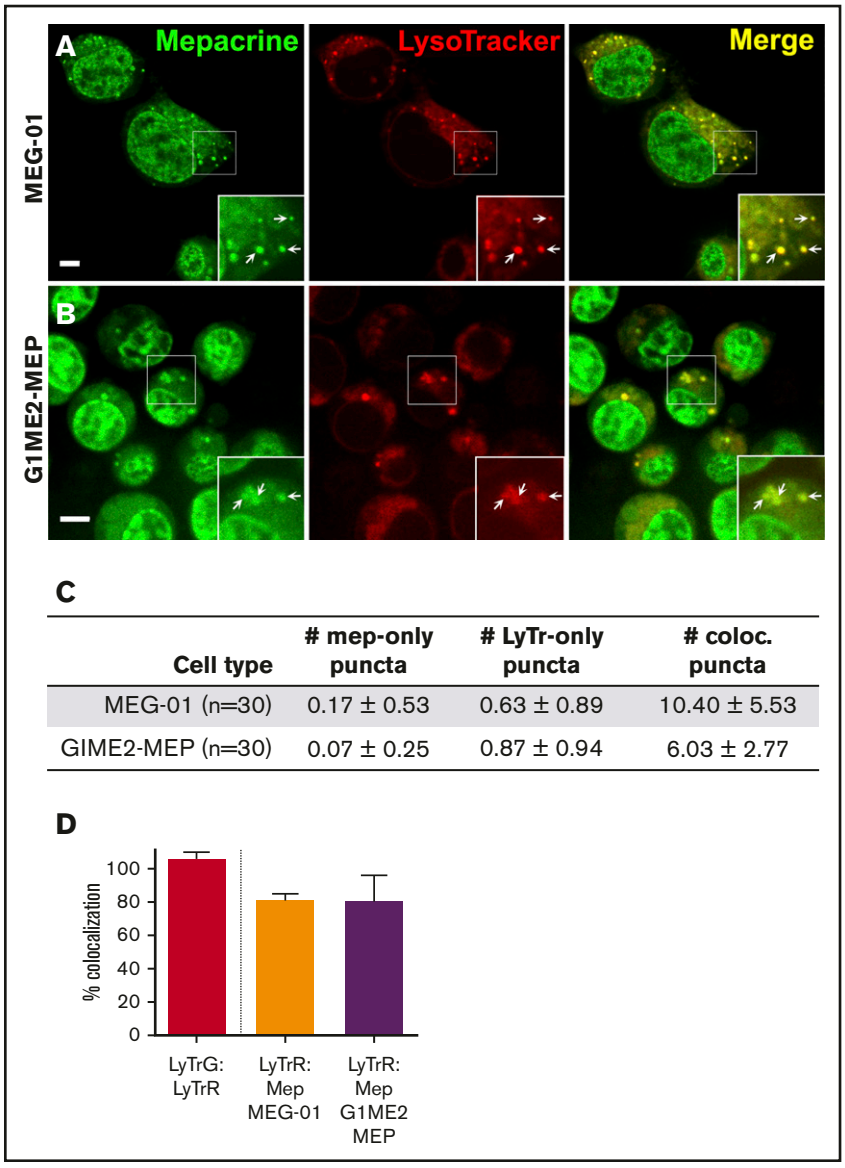

Figure 5. Mepacrine and LysoTracker accumulate in the same compartments in MEG-01 and undifferentiated G1ME2 MK-erythroid progenitors. MEG-01 cells (A,C-D) or G1ME2 MK-erythroid progenitor cells (G1ME2-MEP) (B,C-D) were incubated with 50 μM mepacrine (green) and 200 nM LysoTracker Red DND-99 (red) for 30 min. Images are of a single plane and not deconvolved. Scale bar, 5 μm; ×2 magnifications of boxed regions (insets); examples of overlap (arrows). (C) Quantification of the number (mean ± SD) of puncta per platelet labeled by mepacrine alone (# mep-only), LysoTracker Red alone (# LyTr-only), or both (# coloc.) in 30 cells of each type. (D) Quantification of the percentage (mean ± SD) of mepacrine labeling that colocalized with LysoTracker in MEG-01 (n = 37) and G1ME2-MEP (n = 43) cells, normalized to values for colocalization of LysoTracker Red with LysoTracker Green DND-26 in G1ME2-MK (N = 79), as in Figure 4. MEG-01 cells and G1ME2-MEPs were imaged by spinning-disk confocal microscopy at room temperature with an Ultraview inverted microscope equipped with a 63× Plan Apochromat lens, a Hamamatsu Orca-ER CCD camera, and Volocity software. Imaging medium was IMDM. Mepacrine has an excitation/emission of 436/525 nm; LysoTracker Red excitation/emission: 577/590 nm.

and mechanisms underlying DG maturation and for how diseases such as HPS affect them.

DGs in platelets are characterized as storage compartments for calcium, serotonin, adenine nucleotides, and polyphosphate. Serotonin is also actively incorporated into storage compartments in MKs[26,43-46] by a transporter.[47] If these storage granules are in fact DGs, then we should have observed separate mepacrine-labeled structures in MKs. Our data suggest instead that such structures are not fully matured DGs and are, at the very least, more acidic than they are in platelets. Given that they corresponded to nearly all of the highly acidic structures labeled by LysoTracker dyes in MKs and that they label less densely with mepacrine than do fully matured DGs in platelets,[22] the serotonin storage granules in MKs might actually be acidic endolysosomes. This would be consistent with the accumulation of serotonin and CD63 (a transmembrane protein that is partially enriched in DGs[48]) in multivesicular late endosomes in MKs.[49] It would also be consistent with observations that the platelet-expressed vesicular serotonin transporter, VMAT2,[50] localizes to lysosomal structures that accumulate mepacrine and endocytic tracers and label with the lysosomal membrane protein, LAMP2, in megakaryocytoid MEG-01 cells.[31] VMAT2 and CD63 within late endosomes/lysosomes might ultimately become components of mature DGs either through active transport from these compartments to separate nascent DGs during proplatelet formation or through maturation of the acidic organelles into DGs by activation or deactivation of transmembrane transporters. Alternatively, the serotonin and VMAT2 in these compartments might represent a pool destined for degradation prior to DG formation, consistent with observations that human MKs do not take up serotonin to the same level as platelets[51] and with the model that early endosomes (the compartments within MKs harboring the major cohort of another potential DG cargo protein, SLC35D3[52]) are a primary source for DG membrane contents, as they are for melanosomes in melanocytes.[53] Importantly, our study raises questions about the existence of fully mature DGs in MKs. We speculate that some "bulls-eye"

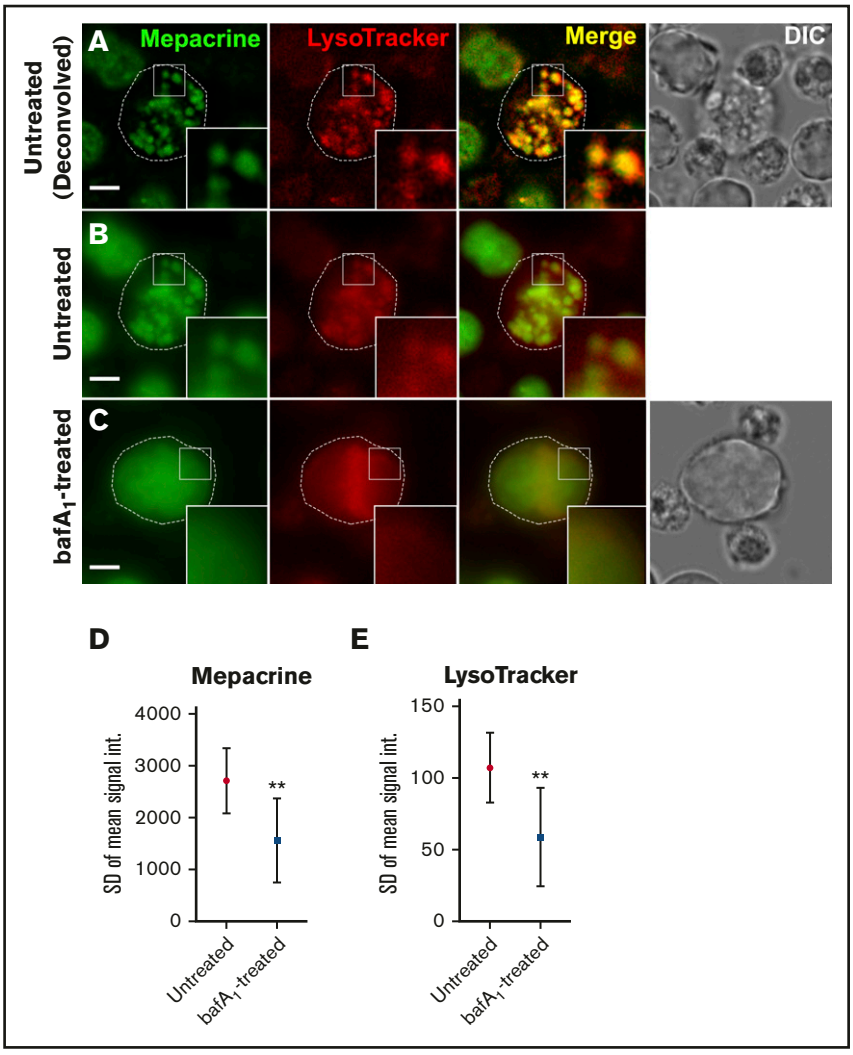

Figure 6. Labeling by mepacrine and by LysoTracker are equally sensitive to deacidification in G1ME2-derived MKs. G1ME2-MKs were pretreated with vehicle alone (untreated) (A-B) or 100 nM bafA$_1$ (C) for 30 min and then labeled with 50 μM mepacrine (green) and 200 nM LysoTracker Red DND-99 for another 30 min in the presence of vehicle or bafA$_1$. Each of the images in panel A are deconvolved from raw, single-plane images shown in panel B; the images in panel C are raw. Corresponding DIC images are shown in panels A and C, and cell outlines based on DIC images are shown by the dotted line. Scale bars, 5 μm; ×2.5 magnifications of boxed region (insets). (D,E) Quantification of the standard deviation in signal intensity of labeling by mepacrine (D) and LysoTracker (E) in vehicle-treated cells (untreated; n = 30) or with bafA$_1$ (n = 30). The difference in signal intensity between treatments was evaluated by unpaired 2-tailed *t* test. G1ME2-MKs were imaged by spinning-disk confocal microscopy at room temperature with an Ultraview inverted microscope equipped with a 63× Plan Apochromat lens, a Hamamatsu Orca-ER CCD camera, and Volocity software. Imaging medium was IMDM. Mepacrine has an excitation/emission of 436/525 nm; LysoTracker Red excitation/emission: 577/590 nm. $^{**}P < .01$. int., intensity.

structures attributed as DGs in MKs by thin-section EM might represent a subtype of α granule, densely stained by heavy-metal ions during EM preparation because of high protein or polyanion content.[10,27,28] Our results suggest that the nature of the acidic mepacrine-labeled structures in cultured MKs must be better understood before considering them as DGs or DG precursors.

Given that mepacrine labels acidic compartments as a weak base in other cell types, it is somewhat surprising that mepacrine strongly and specifically labels DGs in platelets and that this labeling is at least partially insensitive to proton ATPase inhibitors such as bafA$_1$. This suggests that DGs undergo a maturation process whereby mepacrine is either actively pumped into DGs upon maturation or actively retained within DGs. This is consistent with the observation from Reddington et al that mepacrine increases in intensity in platelets in comparison with MKs.[22] Mepacrine might be pumped into DGs via one of the as-yet unidentified transporters for contents such as ADP, serotonin, or calcium, likely in an energy-dependent manner.[39] If this is the case, then the appearance of mepacrine-enriched structures during proplatelet formation might reflect signaling-dependent membrane trafficking of the pump to a precursor organelle or the signaling-dependent activation of a preexisting pump. An intriguing alternative possibility is that mepacrine might be retained within DGs by electrostatic interaction with polyphosphates, which are highly enriched in DGs.[24] This is supported by the cooperative interaction of mepacrine with polyphosphate observed at low ionic strength.[54] Although this ought to be antagonized by the high calcium concentration within DGs, it is possible that activation of additional ion pumps during proplatelet formation might alter the lumenal environment to favor mepacrine: polyphosphate interactions within DGs, deacidification of the organelle, or both. Essentially nothing is known regarding the mechanism of polyphosphate accumulation in DGs, but it is conceivable that polyphosphate generation also begins during proplatelet formation. Distinguishing these possibilities will require a better understanding of DG biogenesis.

If DGs must mature before selective mepacrine uptake takes place, then it is also likely that lysosomes and other acidic organelles change their properties during the transition from MK to proplatelets and platelets. Interestingly, unlike all other cell types examined, LysoTracker-positive compartments in platelets (likely representing lysosomes) did not also label with mepacrine. It is not clear whether this represents a change in properties of the

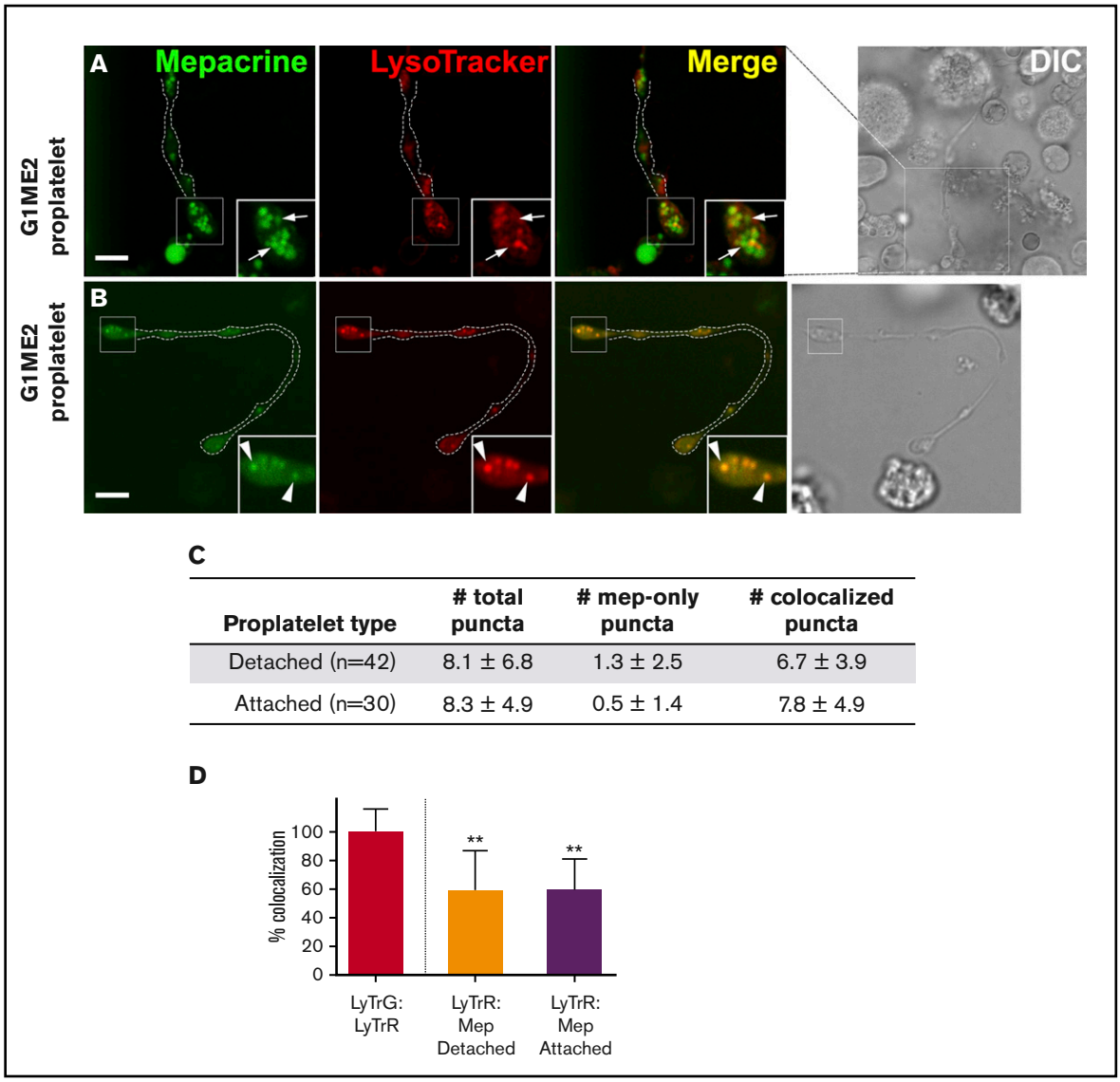

C

Proplatelet type	# total puncta	# mep-only puncta	# colocalized puncta
Detached (n=42)	8.1 ± 6.8	1.3 ± 2.5	6.7 ± 3.9
Attached (n=30)	8.3 ± 4.9	0.5 ± 1.4	7.8 ± 4.9

Figure 7. Structures labeled by mepacrine but not by LysoTracker are first observed in proplatelets. (A-B) G1ME2 cells differentiated for 5-6 days to proplatelets were incubated with 50 μM mepacrine (green) and 200 nM LysoTracker Red DND-99 (red) for 30 min. The panels show raw images of 2 G1ME2-derived proplatelet strings (G1ME2-proplatelet), magnified from the boxed region shown in the corresponding DIC images; the dotted white line in the fluorescent images indicates the outline of the proplatelet from the DIC image. Panel A depicts a proplatelet string with distinct mepacrine-containing compartments (arrows, in insets), and panel B demonstrates a proplatelet string only with puncta that label with both mepacrine and LysoTracker Red (arrowheads, in insets). Scale bars, 5 μm. (C) The number (mean ± SD) of total puncta and puncta labeled by mepacrine alone (mep-only puncta) or by both mepacrine and LysoTracker (coloc. puncta) were quantified per proplatelet string identified as detached or attached as indicated in the text. (D) Quantification of the percentage (mean ± SD) of mepacrine (Mep) labeling colocalized with LysoTracker Red (LyTrR) in detached (n = 42) and attached (n = 30) proplatelets, normalized to 100% for overlap of LysoTracker Red with LysoTracker Green DND-26 (LyTrG) in G1ME2-MK (n = 79). Proplatelets were imaged by spinning-disk confocal microscopy at room temperature with a Leica DMi8 inverted microscope equipped with a Hamamatsu Orca Flash 4 CMOS camera, a 100× Plan Apochromat objective lens (1.4 NA), and VisiVIEW imaging software. Imaging medium was IMDM. Mepacrine has an excitation/emission of 436/525 nm; LysoTracker Red excitation/emission: 577/590 nm. $^{**}P < .01$. int., intensity.

acidic compartments during MK maturation to platelets or simply depletion of the cytoplasmic pool of mepacrine in platelets due to active pumping or retention within DGs. One limitation of our study is the inability to fix mepacrine or Lysotracker to better characterize the labeled compartments in MKs and platelets by immunofluorescence microscopy with antibodies to known endosomal markers. We hope to exploit new live imaging probes to achieve this goal in the future.

If DG maturation coincides with proplatelet formation, then signaling cascades that promote MK maturation and fragmentation into proplatelets likely also stimulate DG maturation. However, although TPO is well established as the main driver of MK differentiation,[55-57] the signals that trigger proplatelet formation are much less characterized. One hypothesis in the field suggests that controlled apoptosis through transient ER stress may initiate thrombopoiesis.[58] It is thus conceivable that the process of DG

maturation might be initiated by activation of ER stress-regulated unfolded response effectors such as IRE1, ATF1, or PERK[59] or by altered activity of kinases, such as mTORC1, that stimulate autophagy.[60] It will be interesting to test whether signaling via one of these effectors ultimately activates AP-3 or BLOC-1, -2 or -3, protein complexes that are deficient in distinct HPS variants and that function during cargo transport to melanosomes in melanocytes.[53]

Acknowledgments

This work was supported by National Institutes of Health, National Heart, Lung, and Blood Institute grants R01 HL121323 (M.S.M.), R01 HL130698 (M.P.), and training grant T32 HL007971 (H.A.H.).

Authorship

Contribution: H.A.H. participated in all aspects of the study and contributed to project conception and experimental design, performed the experiments, analyzed and formatted the data, prepared the figures, and cowrote and edited the manuscript; J.B. contributed to experimental design, performed experiments, analyzed and formatted data, prepared figures, and edited the manuscript; J.-Y.N., D.J., M.P., and M.J.W. contributed to experimental design and edited the manuscript; and M.S.M. conceived of and oversaw the project, contributed to experimental design, oversaw experimental work, performed data analysis, prepared and edited the figures, and cowrote and edited the manuscript.

Conflict-of-interest disclosure: The authors declare no competing financial interests.

ORCID profiles: M.S.M., 0000-0001-7435-7262.

Correspondence: Michael S. Marks, Department of Pathology and Laboratory Medicine, Children's Hospital of Philadelphia, 816G Abramson Research Center, 3615 Civic Center Blvd, Philadelphia, PA 19104; e-mail: marksm@mail.med.upenn.edu.

References

1. Ren Q, Ye S, Whiteheart SW. The platelet release reaction: just when you thought platelet secretion was simple. *Curr Opin Hematol*. 2008;15(5):537-541.
2. Heijnen H, van der Sluijs P. Platelet secretory behaviour: as diverse as the granules … or not? *J Thromb Haemost*. 2015;13(12):2141-2151.
3. Wei AH, Li W. Hermansky-Pudlak syndrome: pigmentary and non-pigmentary defects and their pathogenesis. *Pigment Cell Melanoma Res*. 2013;26(2):176-192.
4. Nurden A, Nurden P. Advances in our understanding of the molecular basis of disorders of platelet function. *J Thromb Haemost*. 2011;9(Suppl 1):76-91.
5. Seward SL Jr, Gahl WA. Hermansky-Pudlak syndrome: health care throughout life. *Pediatrics*. 2013;132(1):153-160.
6. Graham GJ, Ren Q, Dilks JR, Blair P, Whiteheart SW, Flaumenhaft R. Endobrevin/VAMP-8-dependent dense granule release mediates thrombus formation in vivo. *Blood*. 2009;114(5):1083-1090.
7. Meng R, Wu J, Harper DC, et al. Defective release of α granule and lysosome contents from platelets in mouse Hermansky-Pudlak syndrome models. *Blood*. 2015;125(10):1623-1632.
8. Sharda A, Kim SH, Jasuja R, et al. Defective PDI release from platelets and endothelial cells impairs thrombus formation in Hermansky-Pudlak syndrome. *Blood*. 2015;125(10):1633-1642.
9. Stalker TJ, Traxler EA, Wu J, et al. Hierarchical organization in the hemostatic response and its relationship to the platelet-signaling network. *Blood*. 2013;121(10):1875-1885.
10. White JG. Serotonin storage organelles in human megakaryocytes. *Am J Pathol*. 1971;63(3):403-410.
11. White JG. The dense bodies of human platelets: inherent electron opacity of the serotonin storage particles. *Blood*. 1969;33(4):598-606.
12. Da Prada M, Pletscher A. Accumulation of basic drugs in 5-hydroxytryptamine storage organelles of rabbit blood platelets. *Eur J Pharmacol*. 1975;32(02):179-185.
13. Rendu F, Nurden AT, Lebret M, Caen JP. Relationship between mepacrine-labelled dense body number, platelet capacity to accumulate 14C-5-HT and platelet density in the Bernard-Soulier and Hermansky-Pudlak syndromes. *Thromb Haemost*. 1979;42(2):694-704.
14. Skaer RJ, Flemans RJ, McQuilkan S. Mepacrine stains the dense bodies of human platelets and not platelet lysosomes. *Br J Haematol*. 1981;49(3):435-438.
15. Boneu B, Caranobe C, Capdeville J, Robert A, Bierme R. Quantitative evaluation of mepacrine labelled human platelet dense bodies in normals and in cases of peripheral thrombocytopenia. *Thromb Res*. 1978;12(5):831-839.
16. Hourdille P, Bernard P, Reiffers J, Broustet A, Boisseau MR. Platelet dense bodies loaded with mepacrine. Study in chronic idiopathic thrombocytopenic purpura (ITP). *Thromb Haemost*. 1980;43(3):208-210.
17. Rendu F, Breton-Gorius J, Lebret M, et al. Evidence that abnormal platelet functions in human Chédiak-Higashi syndrome are the result of a lack of dense bodies. *Am J Pathol*. 1983;111(3):307-314.
18. Weiss HJ, Lages B, Vicic W, Tsung LY, White JG. Heterogeneous abnormalities of platelet dense granule ultrastructure in 20 patients with congenital storage pool deficiency. *Br J Haematol*. 1993;83(2):282-295.
19. Lorez HP, Richards JG, Da Prada M, et al. Storage pool disease: comparative fluorescence microscopical, cytochemical and biochemical studies on amine-storing organelles of human blood platelets. *Br J Haematol*. 1979;43(2):297-305.

20. Lorez HP, Da Prada M, Rendu F, Pletscher A. Mepacrine, a tool for investigating the 5-hydroxytryptamine organelles of blood platelets by fluorescence microscopy. *J Lab Clin Med*. 1977;89(1):200-206.
21. Lorez HP, Da Prada M. Fluorescence microscopical study of 5-hydroxytryptamine storage organelles in mepacrine-incubated blood platelets of beige mice (Chediak-Higashi syndrome). *Experientia*. 1978;34(5):663-664.
22. Reddington M, Novak EK, Hurley E, Medda C, McGarry MP, Swank RT. Immature dense granules in platelets from mice with platelet storage pool disease. *Blood*. 1987;69(5):1300-1306.
23. Swank RT, Reddington M, Howlett O, Novak EK. Platelet storage pool deficiency associated with inherited abnormalities of the inner ear in the mouse pigment mutants muted and mocha. *Blood*. 1991;78(8):2036-2044.
24. Ruiz FA, Lea CR, Oldfield E, Docampo R. Human platelet dense granules contain polyphosphate and are similar to acidocalcisomes of bacteria and unicellular eukaryotes. *J Biol Chem*. 2004;279(43):44250-44257.
25. White JG. Electron opaque structures in human platelets: which are or are not dense bodies? *Platelets*. 2008;19(6):455-466.
26. Richards JG, Da Prada M. Uranaffin reaction: a new cytochemical technique for the localization of adenine nucleotides in organelles storing biogenic amines. *J Histochem Cytochem*. 1977;25(12):1322-1326.
27. Daimon T, David H. Precursors of monoamine-storage organelles in developing megakaryocytes of the rat. *Histochemistry*. 1983;77(3):353-363.
28. Hourdillé P, Fialon P, Belloc F, Boisseau MR, Andrieu JM. Mepacrine labelling test and uranaffin cytochemical reaction in human megakaryocytes. *Thromb Haemost*. 1982;47(3):232-235.
29. van Nispen tot Pannerden H, de Haas F, Geerts W, Posthuma G, van Dijk S, Heijnen HF. The platelet interior revisited: electron tomography reveals tubular alpha-granule subtypes. *Blood*. 2010;116(7):1147-1156.
30. Pokrovskaya ID, Aronova MA, Kamykowski JA, et al. STEM tomography reveals that the canalicular system and α-granules remain separate compartments during early secretion stages in blood platelets. *J Thromb Haemost*. 2016;14(3):572-584.
31. Ambrosio AL, Boyle JA, Di Pietro SM. Mechanism of platelet dense granule biogenesis: study of cargo transport and function of Rab32 and Rab38 in a model system. *Blood*. 2012;120(19):4072-4081.
32. Allison AC, Young MR. Uptake of dyes and drugs by living cells in culture. *Life Sci (1962)*. 1964;3(12):1407-1414.
33. Noh JY, Gandre-Babbe S, Wang Y, et al. Inducible Gata1 suppression expands megakaryocyte-erythroid progenitors from embryonic stem cells. *J Clin Invest*. 2015;125(6):2369-2374.
34. Denofrio JC, Yuan W, Temple BR, Gentry HR, Parise LV. Characterization of calcium- and integrin-binding protein 1 (CIB1) knockout platelets: potential compensation by CIB family members. *Thromb Haemost*. 2008;100(5):847-856.
35. Fuentes R, Wang Y, Hirsch J, et al. Infusion of mature megakaryocytes into mice yields functional platelets. *J Clin Invest*. 2010;120(11):3917-3922.
36. Rendu F, Maclouf J, Launay JM, et al. Hermansky-Pudlak platelets: further studies on release reaction and protein phosphorylations. *Am J Hematol*. 1987; 25(2):165-174.
37. Handagama PJ, Shuman MA, Bainton DF. Incorporation of intravenously injected albumin, immunoglobulin G, and fibrinogen in guinea pig megakaryocyte granules. *J Clin Invest*. 1989;84(1):73-82.
38. Carty SE, Johnson RG, Scarpa A. Serotonin transport in isolated platelet granules. Coupling to the electrochemical proton gradient. *J Biol Chem*. 1981; 256(21):11244-11250.
39. Dean GE, Fishkes H, Nelson PJ, Rudnick G. The hydrogen ion-pumping adenosine triphosphatase of platelet dense granule membrane. Differences from F1F0- and phosphoenzyme-type ATPases. *J Biol Chem*. 1984;259(15):9569-9574.
40. Heijnen HF, Debili N, Vainchencker W, Breton-Gorius J, Geuze HJ, Sixma JJ. Multivesicular bodies are an intermediate stage in the formation of platelet alpha-granules. *Blood*. 1998;91(7):2313-2325.
41. Handagama P, Rappolee DA, Werb Z, Levin J, Bainton DF. Platelet alpha-granule fibrinogen, albumin, and immunoglobulin G are not synthesized by rat and mouse megakaryocytes. *J Clin Invest*. 1990;86(4):1364-1368.
42. Patel SR, Hartwig JH, Italiano JE Jr. The biogenesis of platelets from megakaryocyte proplatelets. *J Clin Invest*. 2005;115(12):3348-3354.
43. Tranzer JP, da Prada M, Pletscher A. Storage of 5-hydroxytryptamine in megakaryocytes. *J Cell Biol*. 1972;52(1):191-197.
44. Hagen-Aukamp C, Wesemann W, Aumüller G. Intracellular distribution of adenine and 5-hydroxytryptamine in megakaryocytes isolated by density gradient and velocity sedimentation from bone marrow. *Eur J Cell Biol*. 1980;23(1):149-156.
45. Wojenski CM, Schick PK. Development of storage granules during megakaryocyte maturation: accumulation of adenine nucleotides and the capacity for serotonin sequestration. *J Lab Clin Med*. 1993;121(3):479-485.
46. Fedorko ME. The functional capacity of guinea pig megakaryocytes: I. Uptake of 3H-serotonin by megakaryocytes and their physiologic and morphologic response to stimuli for the platelet release reaction. *Lab Invest*. 1977;36(3):310-320.
47. Tytgat GA, van den Brug MD, Voûte PA, Smets LA, Rutgers M. Human megakaryocytes cultured in vitro accumulate serotonin but not meta-iodobenzylguanidine whereas platelets concentrate both. *Exp Hematol*. 2002;30(6):555-563.
48. Westmoreland D, Shaw M, Grimes W, et al. Super-resolution microscopy as a potential approach to diagnosis of platelet granule disorders. *J Thromb Haemost*. 2016;14(4):839-849.
49. Youssefian T, Cramer EM. Megakaryocyte dense granule components are sorted in multivesicular bodies. *Blood*. 2000;95(12):4004-4007.
50. Höltje M, Winter S, Walther D, et al. The vesicular monoamine content regulates VMAT2 activity through Galphaq in mouse platelets. Evidence for autoregulation of vesicular transmitter uptake. *J Biol Chem*. 2003;278(18):15850-15858.

51. Yang M, Srikiatkhachorn A, Anthony M, Chesterman CN, Chong BH. Serotonin uptake, storage and metabolism in megakaryoblasts. *Int J Hematol*. 1996; 63(2):137-142.

52. Meng R, Wang Y, Yao Y, et al. SLC35D3 delivery from megakaryocyte early endosomes is required for platelet dense granule biogenesis and is differentially defective in Hermansky-Pudlak syndrome models. *Blood*. 2012;120(2):404-414.

53. Sitaram A, Marks MS. Mechanisms of protein delivery to melanosomes in pigment cells. *Physiology (Bethesda)*. 2012;27(2):85-99.

54. Zozulya VN, Voloshin IM. Cooperative binding of quinacrine to inorganic polyphosphate. *Biophys Chem*. 1994;48(3):353-358.

55. Cramer EM, Norol F, Guichard J, et al. Ultrastructure of platelet formation by human megakaryocytes cultured with the Mpl ligand. *Blood*. 1997;89(7): 2336-2346.

56. Lecine P, Villeval JL, Vyas P, Swencki B, Xu Y, Shivdasani RA. Mice lacking transcription factor NF-E2 provide in vivo validation of the proplatelet model of thrombocytopoiesis and show a platelet production defect that is intrinsic to megakaryocytes. *Blood*. 1998;92(5):1608-1616.

57. Solar GP, Kerr WG, Zeigler FC, et al. Role of c-mpl in early hematopoiesis. *Blood*. 1998;92(1):4-10.

58. Lopez JJ, Palazzo A, Chaabane C, et al. Crucial role for endoplasmic reticulum stress during megakaryocyte maturation. *Arterioscler Thromb Vasc Biol*. 2013;33(12):2750-2758.

59. Walter P, Ron D. The unfolded protein response: from stress pathway to homeostatic regulation. *Science*. 2011;334(6059):1081-1086.

60. Efeyan A, Comb WC, Sabatini DM. Nutrient-sensing mechanisms and pathways. *Nature*. 2015;517(7534):302-310.